

available at www.sciencedirect.comjournal homepage: www.elsevier.com/locate/carbon

Friction and adhesion properties of vertically aligned multi-walled carbon nanotube arrays and fluoro-nanodiamond films

H. Lu^a, J. Goldman^a, F. Ding^a, Y. Sun^a, M.X. Pulikkathara^b, V.N. Khabashesku^b,
B.I. Yakobson^a, J. Lou^{a,*}

^aDepartment of Mechanical Engineering and Materials Science, Rice University, Houston, TX 77005, United States

^bDepartment of Chemistry, Rice University, Houston, TX 77005, United States

ARTICLE INFO

Article history:

Received 5 November 2007

Accepted 6 May 2008

Available online 15 May 2008

ABSTRACT

Sliding friction and adhesion properties of vertically aligned multi-walled carbon nanotube (VAMWCNT) arrays and fluoro-nanodiamond (F-ND) films on glass substrate have been quantitatively investigated in current study using atomic force microscopy. It was found that VAMWCNT arrays result in lower friction compared to F-ND films. Friction forces were also found to be consistently higher in nitrogen environment than in ambient environment for both samples and a surface chemistry based hypothesis was proposed. However, no apparent dependence of relative humidity was found on adhesion forces for both F-ND and VAMWCNT samples, indicating lack of correlation between nanoscale adhesion and friction. The implications from current study for designing movable components in micro- and nanoelectromechanical system devices were also discussed.

© 2008 Elsevier Ltd. All rights reserved.

1. Introduction

Carbon based materials are known as excellent solid lubricants for many decades. In recent years, carbon nanotubes (CNTs) that possess many unique properties, such as high tensile and flexural strength, high elastic modulus and high aspect ratio, have been explored as promising alternatives for many tribological applications due to the predicted weak intermolecular bonding of CNTs with counter surfaces [1,2]. Additionally, diamond surfaces like diamond-like-carbon (DLC) and nanodiamond (ND) coatings [3,4] also attracted a lot of attentions due to their unrivalled stiffness and hardness, highly adjustable and stable surface chemistry, and excellent macroscale tribological performance. Those carbon based material systems have potential for many advanced technological applications such as sliding interfaces between moving components in micro- and nano-electro-mechanical systems (MEMS/NEMS).

Despite their exciting prospects in nanotribological applications, there have been only a few theoretical and experimental studies on CNT friction properties. Ni and Sinnott [5] used many-body empirical potential for hydrocarbons coupled to Lennard-Jones potentials in their molecular dynamic simulations to study friction between SWCNT bundles and hydrogen terminated diamond surfaces. They showed that the friction force is not linear to the applied normal load, unlike the prediction by Amontons–Coulomb friction law at the macro-scale, and the friction coefficient is not well defined at the nanometer scale. Hirata and Yoshioka [6] studied sliding friction properties of microwave-plasma-enhanced chemical vapor deposition (MPCVD) deposited CNTs on different substrates by means of steel ball-on-disk type of testing. Based on friction coefficient measurements, they found that friction force was reduced when CNTs had less defects and higher crystallinity, and also when tests were conducted in vacuum. Tu et al. [7] used both atomic force microscope (AFM) and a

* Corresponding author. Fax: +1 713 348 5423.

E-mail address: jlou@rice.edu (J. Lou).

0008-6223/\$ - see front matter © 2008 Elsevier Ltd. All rights reserved.

doi:10.1016/j.carbon.2008.05.010

ball-on-disk tribometer for friction study of carbon nanotubes embedded in anodic aluminum oxide template. Contrary to earlier theoretical study [5], they found a linear relationship between friction force and normal load in their nanoscale AFM based tests, and a decrease of friction coefficient (0.12–0.08) with increasing sliding velocity from 0.04 m/s to 0.16 m/s in their ball-on-disk based tests [7]. Kinoshita et al. [8] showed very high friction coefficients of 1.0–2.2 for vertically aligned carbon nanotube forests with 6 μm length against gold tips of different radii. Dickrell et al. [9,10] studied multi-walled CNT films oriented in two orthogonal directions using a micro-tribometer and found extremely high friction coefficient for vertically aligned CNT films and very low friction coefficient for CNT dispersed transversely on the same substrates. They also demonstrated the strong effects of surface chemistry and temperature on friction behaviors of both vertically and transversely oriented CNT films. Lou and Kim [11] employed AFM using both bare and aluminum coated colloidal probes (with 15 μm diameter borosilicate sphere attached to the end of regular AFM cantilever) to study effects of interfaces on friction behavior of vertically aligned carbon nanotube arrays, and found much higher friction forces for aluminum coated colloidal probes compared to bare borosilicate colloidal probes.

Similarly for diamond surfaces, there are not many systematical studies undertaken on their tribological properties especially at the nanometer scale. Carpick et al. [3] studied the effects of relative humidity on nanoscale adhesion and friction behavior of DLC films on Si substrates deposited by ion deposition process. They found that friction force consistently rose with the increasing relative humidity providing an excellent fit of their experimental data with the Derjaguin–Müller–Toporov (DMT) model. Sumant et al. [4] investigated the nanotribological properties of the underside of ultrananocrystalline diamond (UNCD) film grown on Si substrate by MPCVD. AFM based friction measurements revealed that both friction and adhesion of UNCD film reduced after hydrogen termination treatment.

In this paper, the frictional and adhesion behaviors of two carbon based nanostructured surfaces were quantitatively investigated using AFM for direct comparison. Effects of relative humidity on friction and adhesion were thoroughly investigated in a chamber with well-controlled environment for both VAMWCNT arrays and F-ND films on glass substrate.

2. Materials and experimental procedures

2.1. Sample preparation

2.1.1. Vertically aligned multi-walled carbon nanotube (VAMWCNT) arrays

Highly ordered arrays of VAMWCNT embedded in a hexagonal close-packed alumina template were grown by chemical vapor deposition (CVD) technique [12]. The as-grown vertically aligned multi-walled carbon nanotubes (VAMWCNT) arrays fully embedded in the nanoporous alumina template were then partially exposed by etching the alumina matrix to desired depth. For samples used in the current study, MWCNT arrays with 30 nm protruded length were prepared. The

diameter of these MWCNTs is about 25–40 nm with \sim 50 nm inter-channel distance. A topological AFM scan of the sample surface before the experiments is shown in Fig. 1a.

2.1.2. Fluoro-nanodiamond (F-ND) films

A method for direct fluorination of nanodiamond (ND) powder to produce fluoro-ND has been developed at Rice University [13]. Commercially available nanoscale diamond powder (Nanostructured and Amorphous Materials, Inc.; >97% purity) of about 4 nm average particle size prepared by detonated explosion synthesis was used in the present study. After fluorination of ND powder at 310 $^{\circ}\text{C}$, the obtained F-ND nanoparticles have been covalently bonded to an oxidized and subsequently 3-aminopropyl(triethoxy) silane-modified glass substrate through wet chemistry reaction. By using this innovative and simple approach, a 10–40 nm thick and transparent nanodiamond films on glass have been fabricated [14]. The covalent bonding of ND to glass substrate has been verified by ultrasonication in ethanol, causing no debonding of F-ND from the substrate, and by XPS surface analysis. The surface morphology of the F-ND film was characterized by AFM under contact mode (Fig. 1b).

2.2. Experimental procedures

AFM and Lateral Force Microscopy (LFM) studies were performed on both VAMWCNT array and F-ND film samples. A Pico-plus AFM (Agilent AFMs, Tempe, Arizona) with a silicon AFM probe was used in this study. The AFM/LFM scans were performed with progressively decreasing normal load for every 20 scans or so, this was done to measure the encountered friction force as a function of the applied normal load. Both VAMWCNT and F-ND samples were scanned at several different locations to ensure the proper representation of the sample surface. Scans were also repeated over the exact same location to check the reproducibility of the experiment. Pre and after scans were performed to ensure no damage to sample surfaces occurred during our experiments. The test was run with a scan size of 1 μm using the small scanner (maximum scan size 9 μm) at scan speed of 2000 nm/s.

In order to quantify the adhesion forces between sample surfaces and the AFM probe, force vs. distance spectroscopy was run on both samples and the amount of adhesion was measured. A robust procedure has also been developed in this study to construct an adhesion force map consisting of 1024 force-distance spectroscopy curves in each scan to characterize adhesion characteristics of the samples with proper statistical treatments.

Humidity of the testing environment was controlled using a plastic environmental isolation chamber which separates the AFM from the ambient conditions (relative humidity larger than 60%). Controlled flow of nitrogen gas was used to create dry environment with relative humidity less than 5%. Both relative humidity and temperature were monitored using a digital hygrometer/thermometer before, during and after the actual testing. Temperature was found to vary negligibly during all of our experiments. Table 1 shows typical testing conditions for our adhesion and friction experiments under both dry and ambient environments.

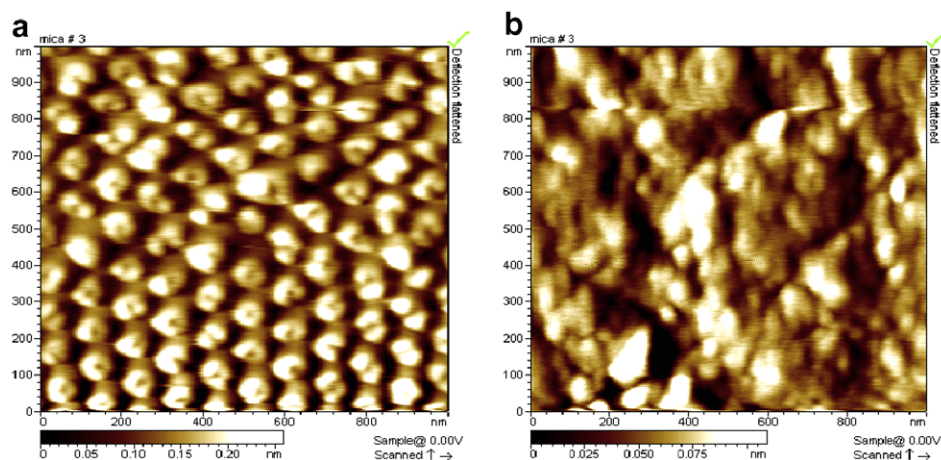


Fig. 1 – (a) AFM scan of the VAMWCNT arrays with 30 nm protruded length and (b) AFM scan of the F-ND films on glass substrates.

Table 1 – Typical testing conditions demonstrate well-controlled environments

Samples	RH % (Ambient)		RH % (Dry)		Temperature (F) (Ambient)		Temperature (F) (Dry)	
	Before	After	Before	After	Before	After	Before	After
VAMWCNT Arrays	62.6	62.3	0.8	3.8	65.5	65.5	66.4	66.5
F-ND films	63.4	64.6	1.2	2.8	65.6	65.6	66.7	66.7

It should be noted here, although AFM has been widely used for studying nano-scale interaction forces ever since its invention [15–18], one of the biggest challenges of using AFM for quantitative nanomechanical measurements remains to be reliable conversion from the position sensitive photodiode (PSPD) readout (voltage) to actual force exerted or experienced by the AFM probe during tip-sample interaction. For normal direction force calibration, it is now becoming standard practice to use a pre-calibrated cantilever with known stiffness (e.g. CLFC-NOBO from veecoprobes.com) to calibrate force constant *in situ*. For more problematic lateral direction force calibration, we have adopted a novel friction force calibrator based on diamagnetic levitation in current study. A diamagnetically levitated pyrolytic graphite (PG) sheet covered by an atomically flat mica sheet was used as a “magnetic” spring, to directly correlate the applied lateral force on the AFM probe with the output voltage signal generated by PSPD. This *in situ* procedure provides a simple and reliable way for AFM based friction force calibration with high accuracy and effectiveness, making it possible to quantitatively study the nano-friction behavior in a reproducible manner. The details of this method have been discussed elsewhere [19]. Both normal and lateral force calibrations were carefully performed *in situ* before each experiment in order to get quantitative measurements for adhesion and friction forces.

3. Results

3.1. Friction properties

Fig. 2a shows the variation of lateral force (friction) with applied normal load for VAMWCNT array sample in an envi-

ronment of ambient conditions (with RH $\sim 63\% \pm 1.5\%$ throughout the experiments for all cases) and dry conditions (with RH $< 5\%$ throughout the experiments for all cases). As can be seen from Fig. 2a, data from multiple tests scatter quite significantly at both humidity levels. This reflects the heterogeneous nature and relatively high roughness of the VAMWCNT array sample surfaces. Despite the data scattering, friction is clearly higher in dry nitrogen condition than in ambient condition. The pull-off force (force at which the AFM tip pulls out of contact from sample surface and the later force goes to zero) is quite similar for both conditions and does not go to negative (adhesive) side.

Similarly, friction properties of F-ND films on glass substrates plotted against normal load are shown in Fig. 2b for both ambient and dry conditions. Data from multiple tests overlap very closely at each relative humidity level as also observed previously for DLC films deposited on Si substrates [3]. This implies relatively smooth surfaces for F-ND samples. Again, we clearly observed higher friction in dry nitrogen condition than in ambient condition. Unlike VAMWCNT array samples, adhesive component is apparent for the measured pull-off forces.

Finally, it is worth noting that VAMWCNT arrays generally result in lower friction compared to F-ND films at both humidity levels (Fig. 3). Upon close inspection, the difference in friction appears to be larger for samples tested in ambient environment at higher normal load, while it is the opposite trend for samples tested in dry nitrogen environment as shown in Fig. 3. In addition, the friction difference for VAMWCNT arrays tested at the two humidity levels is greater than that for F-ND films.

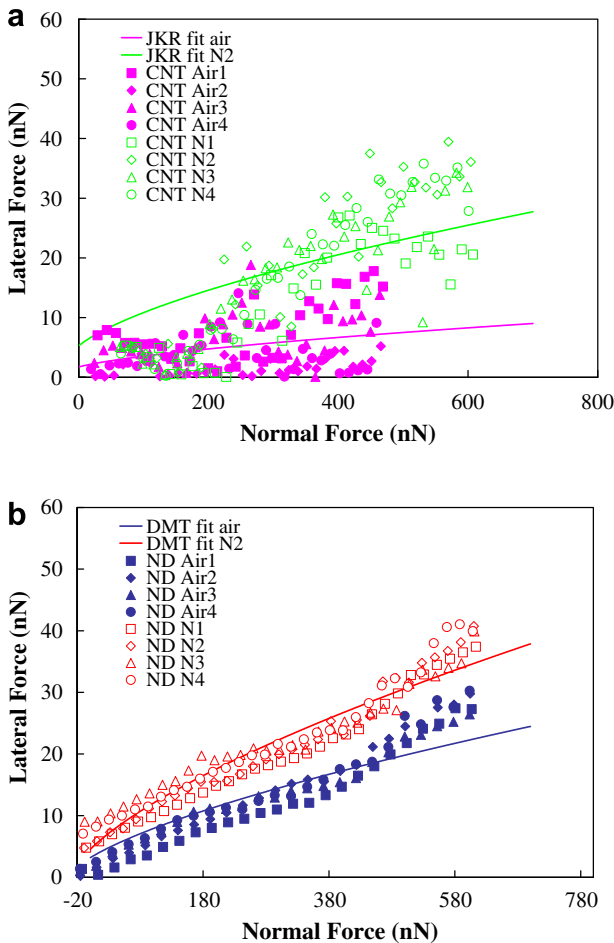


Fig. 2 – (a) Friction vs. applied normal load at ambient and dry conditions for VAMWCNT array samples. Solid lines: JKR fit (b) Friction vs. applied normal load at ambient and dry conditions for F-ND films on glass substrate. Solid lines: DMT fit.

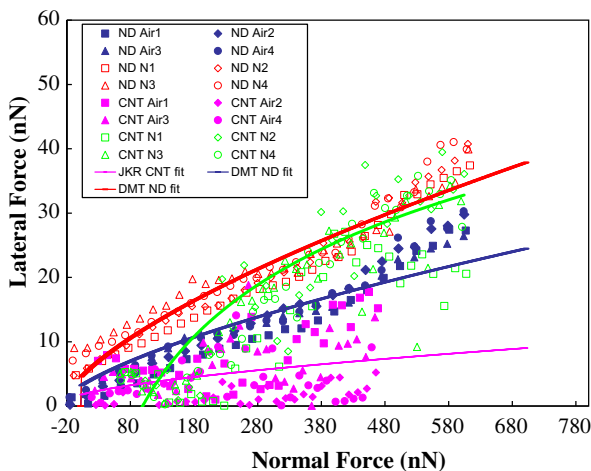


Fig. 3 – Comparison of friction vs. applied normal load curves for both VAMWCNT array and F-ND samples at ambient and dry conditions (trend line was adopted for VAMWCNT samples tested under dry nitrogen condition due to poor JKR fit).

3.2. Adhesion properties

In order to better quantify the adhesive forces between the AFM probe and samples surfaces, adhesive force mapping was carried out for both VAMWCNT and F-ND samples in the same well-controlled environments. Fig. 4a shows a typical three dimensional adhesive force map for VAMWCNT array samples with 1024 force-spectroscopy measurements performed in ambient conditions, the corresponding histogram for the measured adhesive forces is shown in Fig. 4b. Similar data was also collected for VAMWCNT samples in dry nitrogen environment (Figs. 4c and d). Note that such adhesive force mapping was performed at random locations on sample surfaces to get the general representation of their surface properties. The average adhesive forces between VAMWCNT array samples and AFM probe are almost indistinguishable, 23.5 ± 12 nN in ambient environment and 28.1 ± 13 nN in dry nitrogen environment, considering their statistical variations. This is in sharp contrast with the strong dependence of friction properties on relative humidity seen earlier that clearly indicates the lack of correlation between friction and adhesion properties at the nanoscale. Similarly, adhesive force mapping procedure was repeated for F-ND film on glass substrate at both humidity levels. Typical three dimensional adhesive force maps, obtained in ambient and nitrogen environments, are shown in Figs. 5a and c along with corresponding histogram for measured adhesive forces in Figs. 5b and d. Again, there is little difference between average adhesive force in ambient (30.2 ± 6 nN) and dry nitrogen environments (28.3 ± 7 nN). Comparison with Fig. 3 which shows that friction behavior of the same samples is clearly dependent on relative humidity level, the lack of correlation between nanoscale friction and adhesion is again very evident.

4. Discussions

Generally, the friction force F can be described by a dependence of true contact area A and the interfacial shear strength τ for nanoscale single asperity contacts:

$$F = \tau \cdot A \tag{1}$$

From contact mechanics theory, Hertz obtained the following relationship relating the contact area A with the normal load L assuming no attractive forces acting between the two materials:

$$A = \pi \left(\frac{R}{K} L \right)^{2/3} \tag{2}$$

where R is tip radius and K is the contact modulus, defined as

$$K = \frac{4}{3} \left(\frac{1 - \nu_{\text{tip}}^2}{E_{\text{tip}}} + \frac{1 - \nu_{\text{sample}}^2}{E_{\text{sample}}} \right)^{-1} \tag{3}$$

Besides Hertz theory of contact, Johnson–Kendall–Roberts (JKR) theory Eq. (4b) predicts the relationship between contact area and normal load for relatively compliant materials and strong adhesive forces whereas Derjaguin–Muller–Toporov (DMT) theory Eq. (4b) works for relatively stiff materials and weak adhesive forces:

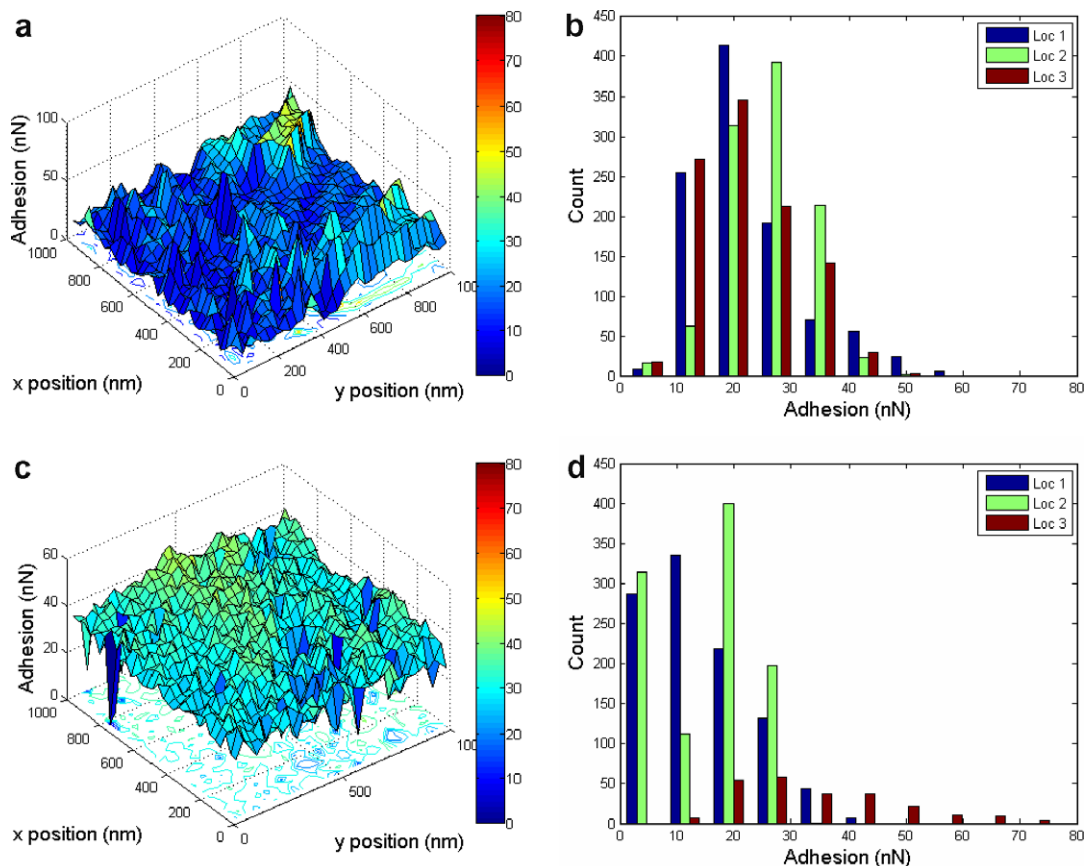


Fig. 4 – (a) Typical three dimensional adhesive force map of VAMWCNT array sample in ambient environment, (b) Corresponding histogram for measured adhesive forces at independent locations, (c) Typical three dimensional adhesive force map of VAMWCNT array sample in nitrogen environment and (d) Corresponding histogram for measured adhesive forces at independent locations (Scan size: 1 μm).

$$A = \pi \left(\frac{R}{K} \left(L - 2L_c + \sqrt{4L_c(L_c - L)} \right) \right)^{2/3} \quad (4a)$$

$$A = \pi \left(\frac{R}{K} (L + L_c) \right)^{2/3} \quad (4b)$$

where L_c is the critical load required to pull the tip off from the sample surface (the adhesive pull-off force). If the interfacial shear strength τ is assumed to be constant, then above solutions for contact area can be directly fitted to the friction data obtained earlier in Figs. 2 and 3. In our fitting process, we let the radius of the AFM tip and the contact modulus to be free parameters. Since adhesive forces are carefully measured for all of the samples studied, we used both JKR and DMT theory to fit the results obtained for both VAMWCNT array sample and F-ND film samples. It was found JKR theory generally works better for VAMWCNT sample and DMT theory also works better for F-ND film sample as expected. However, as clearly indicated in Fig. 2, the relationship between the measured friction force and the contact area for VAMWCNT array samples in ambient environment is not well predicted by the JKR theory. This apparent deviation from JKR prediction especially at low normal load is currently under investigation. While for samples tested under other conditions (Figs. 2 and 3), JKR and DMT theories seem to work reasonably well.

Finally, it is worth noting that the AFM tip radius used in our study is ~ 40 nm as determined independently from scanning the tip over an array of sharp tips and if the contact modulus is known, the interfacial shear strength could be extracted from the fit for both samples.

In addition, our experiments showed the lack of any changes in adhesion as function of relative humidity level while quite significant changes in friction under similar conditions for both samples. This weak dependence of adhesion on humidity and lack of correlation between adhesion and friction may not be a singular case at the nanoscale, as it has been observed before in other systems [3,20–22]. One direct implication of this phenomenon is that the classical meniscus theory may no longer be applicable since it predicts substantial variation of adhesion with humidity. The relatively hydrophobic nature of the fluorinated ND film and VAMWCNT array samples could have prevented the accumulation of water molecules on their surface to reach a minimum thickness needed to form the water meniscus. However, without direct experimental analysis of the interfacial chemistry and structure performed *in situ* at the nanoscale, it is too early to rule out the possible important role played by water molecules.

Finally, it is evident from our experiments that friction is clearly higher at lower relative humidity level. This is very

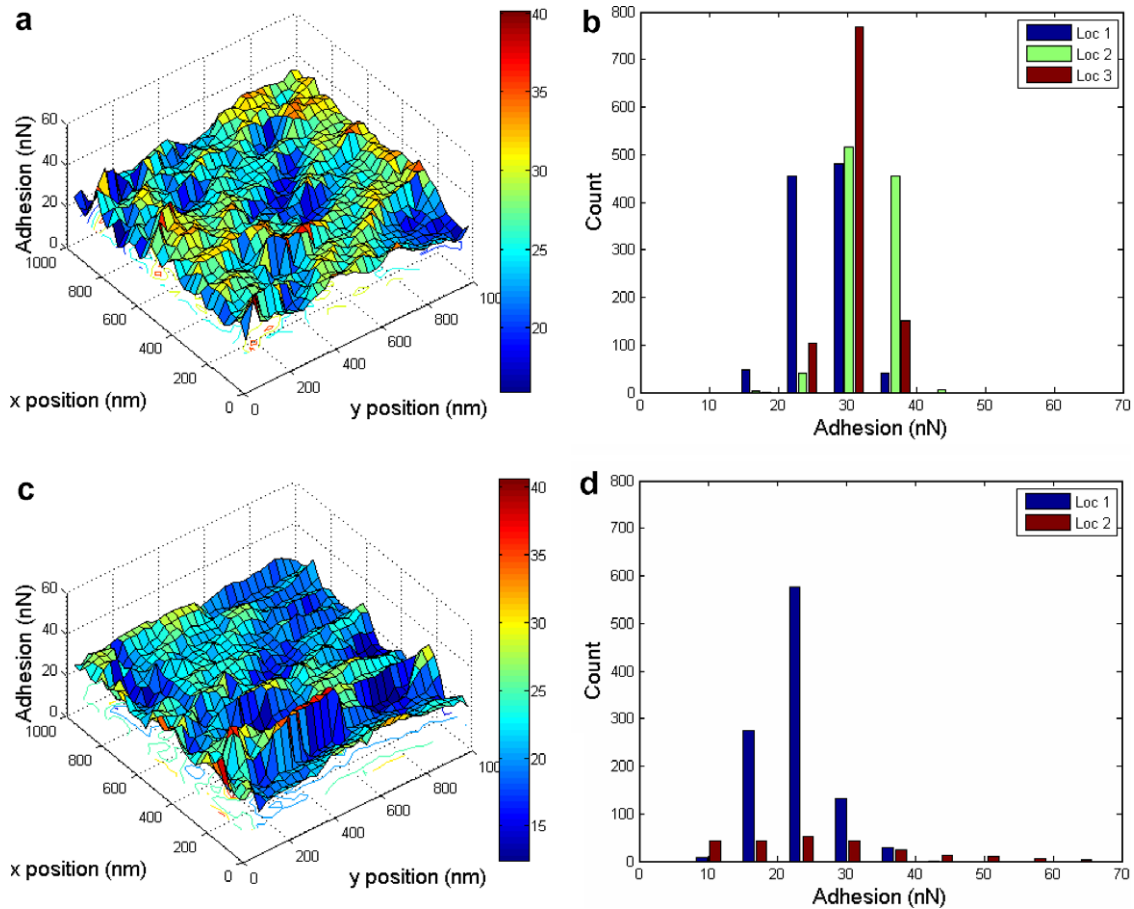


Fig. 5 – (a) Typical three dimensional adhesive force map of F-ND film on glass substrate in ambient environment, (b) Corresponding histogram for measured adhesive forces at independent locations, (c) Typical three dimensional adhesive force map of F-ND film on glass substrate in ambient environment and (d) Corresponding histogram for measured adhesive forces at independent locations (Scan size: 1 μ m).

different from earlier nano-scale friction study of DLC films prepared by ion deposition process where they find friction increase as relative humidity level goes up [3], and also the micro-scale friction study of vertically aligned carbon nano-

tubes in air and argon environments where they found lower friction coefficient at lower humidity level [9]. One possible answer has been offered by friction study between two mica surfaces or two amorphous carbon films using surface force

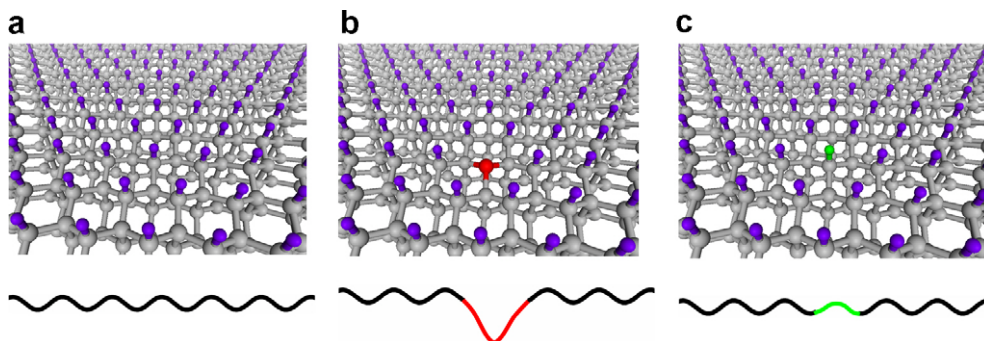


Fig. 6 – A fully fluorinated diamond surface (a) and a fluorinated diamond surface with an active site (e.g., carbon dangling bond shown in red in b). The dangling bond was passivated by a hydrogen atom and thus the active site was annihilated (c). The F atoms are shown in purple, C atoms are shown in gray and red, and the H is shown in green. The corresponding potential energy profiles are shown in the bottom of each figure.

apparatus at different humidity level [23]. Formation of a very thin water film at these interfaces was thought to decrease the effective contact area and serve as a very good lubricant to reduce friction. However, the existence of the water film would naturally cause a strong dependence of adhesion as a function of humidity level which is not true in current study as pointed out earlier.

Another plausible explanation could be saturation of the carbon dangling bonds at active sites on sample surfaces by chemisorption of water molecules. We believe roughness of the sample surface and the extent of the adhesion present between the sample surface and the AFM probe are two important factors affecting nano-scale friction behavior studied in current work. More active sites with dangling bonds (which normally cause high adhesion between AFM probes and surfaces) result in high friction for surfaces with same roughness. Certainly, the only possible difference between friction measurements made at ambient condition and dry nitrogen condition for the same sample surface is originated from the extent of the adhesion existing between the sample surface and the AFM probe interface. In ambient conditions, an active water molecule can be easily dissociated into H^+ and OH^- , and the H^+ can be easily attracted to an active site of the surfaces (e.g., a carbon dangling bond site on F-ND surface as shown in Fig. 6) and passivate it. On the other hand, in pure nitrogen condition, due to the lack of active water molecules, the unpassivated sites will increase the friction force. Based on this postulation, the significant friction difference of VAMWCNT samples at ambient condition and nitrogen condition in contrast to the smaller difference of F-ND films observed in Fig. 3 can be understood by the concentration difference of the active sites on VAMWCNT tip and F-ND surface: since the ND are fluorinated before the measurement, the active site concentration should be significantly lower than that on the VAMWCNT tip. Whereas normally only very small fraction of the active sites on both VAMWCNT tip and F-ND surface are not passivated (although the concentration difference between them is large), so the adhesion force measured by point-to-point force spectroscopy mapping does not change so much at different conditions. While this interpretation is still largely speculative at the moment, detailed molecular dynamic simulation is underway to shed lights on understanding of this interesting phenomenon.

5. Summary

In summary, a quantitative study of friction and adhesion properties was performed on VAMWCNT arrays and F-ND films on glass substrates in both ambient and dry environments. Contact mechanics based theories were able to provide a reasonable fit to nano-friction experimental data in most cases. VAMWCNT arrays consistently generated lower friction at both humidity levels compared to F-ND films. Friction forces were also found to be higher in nitrogen environment than in air for both samples while no apparent dependence on relative humidity was found for adhesion forces, indicating the lack of correlation between nanoscale adhesion and friction. A surface chemistry based hypothesis was proposed to explain the experimental observations.

Acknowledgements

The authors gratefully acknowledge the support from the Center for Biological and Environmental Nanotechnology (NSF Award EEC-0647452). This material is also based on research sponsored by Air Force Research Laboratory under agreement number FA8650-07-2-5061. MXP and VNK would like to acknowledge NASA-ARC Graduate Student Research Program and the U.S. Civilian Research and Development Foundation for Independent States of the Former Soviet Union (Award No. RUE 2-2659-MO-05).

REFERENCES

- [1] Salvétat-Delmotte JP, Rubio A. Mechanical properties of carbon nanotubes: a fiber digest for beginners. *Carbon* 2002;40(10):1729–34.
- [2] Van der Wall RL, Miyoshi K, Street KW, Tomasek AJ, Peng H, Liu Y, et al. Friction properties of surface-fluorinated carbon nanotubes. *Wear* 2005;259:738–43.
- [3] Carpick RW, Flater EE, Sridharan K. The effect of surface chemistry and structure on nano-scale adhesion and friction. *Polym. Mater.* 2004;90:197–8.
- [4] Sumant AV, Grierson DS, Gerbi JE, Birrell J, Lanke UD, Auciello O, et al. Toward the ultimate tribological interfaces: surface chemistry and nanotribology of ultrananocrystalline diamond. *Adv. Mater.* 2005;17(8):1039–45.
- [5] Ni B, Sinnott SB. Tribological properties of carbon nanotube bundles predicted from atomistic simulations. *Surf. Sci.* 2007;487(April):87–96.
- [6] Hirata A, Yoshioka N. Sliding friction properties of carbon nanotube coatings deposited by microwave plasma chemical vapor deposition. *Tribol. Int.* 2004;37(11–12):893–8.
- [7] Tu JP, Jiang CX, Guo SY, Fu MF. Synthesis and frictional properties of array film of amorphous carbon nanofibers on anodic aluminum oxide. *Carbon* 2004;41:1257–63.
- [8] Kinoshita H, Kume I, Tagawa M, Ohmae N. High friction of a vertically aligned carbon-nanotube film in microtribology. *Appl. Phys. Lett.* 2004;85:2780–1.
- [9] Dickrell PL, Sinnott SB, Hahn DW, Raravikar NR, Schadler LS, Ajayan PM, Sawyer WG. Frictional anisotropy of oriented carbon nanotube surfaces. *Tribol. Lett.* 2005;18:59–62.
- [10] Dickrell PL, Pal SK, Bourne GR, Muratore C, Voevodin AA, Ajayan PM, Schadler LS, Sawyer WG. Tunable friction behavior of oriented carbon nanotube films. *Tribol. Lett.* 2006;24:85–90.
- [11] Lou J, Kim KS. Effects of interfaces on nano-friction of vertically aligned multi-walled carbon nanotube arrays. *Mater. Sci. Eng. A* 2008;483–484:664–7.
- [12] Li J, Papadopoulos C, Xu JM. Highly ordered carbon nanotube arrays for electronics applications. *Appl. Phys. Lett.* 1999;75:367–9.
- [13] Liu Y, Gu Z, Margrave JL, Khabashesku VN. Functionalization of nanoscale diamond powder: fluoro-, alkyl-, amino- and aminoacid-nanodiamond derivatives. *Chem. Mater.* 2004;16:3924–30.
- [14] Liu Y, Khabashesku VN, Halas NJ. Fluorinated nanodiamond as a wet chemistry precursor for diamond coatings covalently bonded to glass surface. *J. Am. Chem. Soc.* 2005;127:3712–3.
- [15] Binnig G, Quate CF, Berber C. Atomic force microscope. *Phys. Rev. Lett.* 1986;56:930–3.

-
- [16] Mate CM, McClelland GM, Erlandsson R, Chiang S. Atomic-scale friction of a tungsten tip on a graphite surface. *Phys. Rev. Lett.* 1987;59:1942–5.
- [17] Carpick RW, Agrait N, Ogletree DF, Salmeron MJ. Measurement of interfacial shear (friction) with an ultrahigh vacuum atomic force microscope. *Vac. Sci. Technol.* 1996;B14:1289–95.
- [18] Perry SS. Scanning probe microscopy measurements of friction. *MRS Bull.* 2004;29(7):478–83.
- [19] Li Q, Rydberg A, Kim KS. Lateral force calibration of an atomic force microscope with a diamagnetic levitation spring system. *Rev. Sci. Instr.* 2006;77:065105-1-13.
- [20] Xu L, Lio A, Hu J, Ogletree DF, Salmeron M. Wetting and capillary phenomena of water on mica. *J. Phys. Chem. B* 1998;102:540–8.
- [21] Xiao X, Qian L. Investigation of humidity-dependent capillary force. *Langmuir* 2000;16:8153–8.
- [22] He M, Blum AS, Aston DE, Buenviaje C, Overney RM, Luginbuhl R. Critical phenomena of water bridges in nanoasperity contacts. *J. Chem. Phys.* 2001;114:1355–60.
- [23] McGuiggan PM, Hsu SM, Fong W, Bogy D, Bhatia CS. Friction measurements of ultra-thin carbon overcoats in air. *J. Tribol.* 2002;124:239–44.